

## Charts for water hammer in low head pump discharge lines resulting from water column separation and check valve closure

EUGEN RUUS, BRYAN KARNEY, AND FAROUK A. EL-FITANY

*Department of Civil Engineering, University of British Columbia, Vancouver, B.C., Canada V6T 1W5*

Received January 13, 1984

Revised manuscript accepted June 13, 1984

Maximum pressure head rises resulting from water column separation and check valve closure are calculated and plotted for a simple low head pump discharge line with one well-defined high point. Basic parameters such as pipeline constant, pipe wall friction, complete pump characteristics, pump inertia constant, and the relative location of the high point are accounted for in the analyses. The results of this paper can be used to determine (a) when water column separation is expected, (b) how to avoid water column separation, and (c) the necessary wall thickness in cases where no protection against water column separation is provided. Computer studies indicate that both the vertical and horizontal location of the high point as well as the pipe friction, the pipeline constant, and the pump inertia have a major effect on pressure head rises. Water column separation does not always constitute a danger to the pipeline.

*Key words:* waterhammer, water column separation, check valve closure, pressure rise, pump discharge line, chart.

Les surpressions maximales résultant de la séparation de la colonne d'eau et de la fermeture d'un clapet de retenue sont calculées et mises en graphiques dans le cas d'une conduite simple, comportant un point haut bien défini, alimentée par une pompe développant une faible hauteur de charge. L'analyse tient compte des paramètres fondamentaux tels que la constante de la conduite, le frottement à la paroi, l'ensemble des caractéristiques de la pompe, la constante d'inertie de la pompe et la position relative du point haut de la conduite. Les résultats contenus dans cet article peuvent être utilisés pour déterminer: (a) sous quelles conditions la séparation de la colonne d'eau est susceptible de se produire, (b) comment éviter la séparation de la colonne d'eau et (c) l'épaisseur de paroi requise dans les cas où il n'existe aucune protection contre la séparation de la colonne d'eau. Les études montrent que les coordonnées verticale et horizontale du point haut de même que le frottement dans la conduite, la constante de la conduite et l'inertie de la pompe jouent un rôle important dans la valeur de la surpression. La séparation de la colonne d'eau ne constitue pas toujours un danger pour la conduite.

*Mots clés:* conduite de refoulement d'une pompe, coup de bélier, diagrammes, fermeture de clapet, séparation d'une colonne d'eau, surpression.

[Traduit par la revue]

Can. J. Civ. Eng. 11, 717-742 (1984)

### Introduction

Water column separation is likely to occur when pumps fail in an unprotected low head installation that has a long pipeline carrying water at high velocity. Many pipe failures in low head installations have been directly ascribed to water column separation as the main cause or as the aggravating condition that led to the failure. It is therefore of interest to know which circumstances produce water column separation and what the resulting maximum pressure rise would be. In low head installations the steady state pressure head is often only a fraction of the allowable pressure head, the minimum pipe wall thickness being determined by considerations of wear, corrosion, handling, etc. It may therefore be more economical in some cases to make the pipe strong enough to withstand the consequences of water column separation, rather than making provisions to avoid the column separation.

When the minimum total pressure head at a point along the pipe falls to vapour pressure head, water column separation is initiated. The minimum total head

is obtained by subtracting the largest pressure head drop from the initial steady state pressure head. The pressure head drop is caused by the pump slowdown and the corresponding discharge reduction during the down-surge condition that is initiated by power failure. It follows that for a given velocity reduction and the resulting pressure head drop, the vapour pressure is more likely reached with a lower initial head than with a higher one. Therefore low head installations are more susceptible to water column separation than high head installations.

Water column separation is most likely to occur in a knee in the profile in an unprotected pipeline. A sketch of a typical pump installation involving a high point is shown in Fig. 1.

Upon power failure, the speed of the pump, the discharge through the pump, and the pumping head decrease rapidly. When the vertical distance between the falling hydraulic grade line EDFW and the point A reaches approximately 9.6 m (31.50 ft) water column separation is initiated at this point. The cavity forming

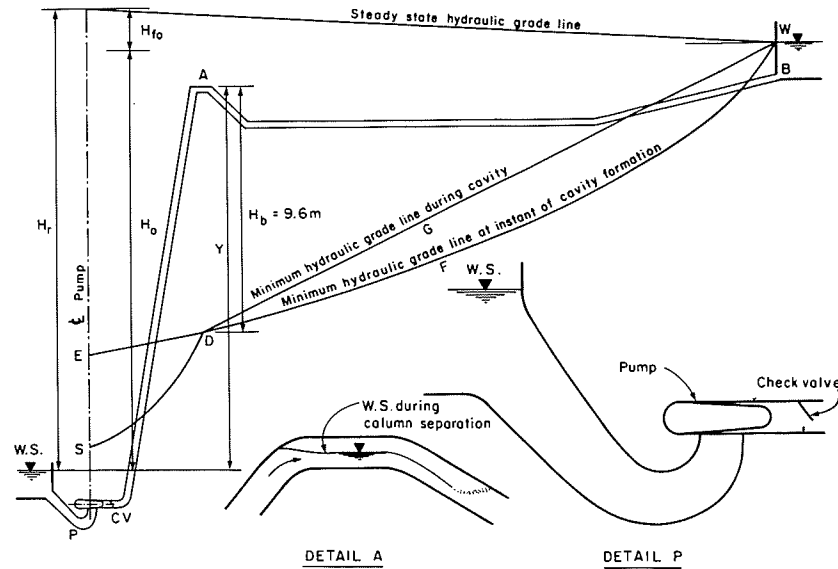


FIG. 1. Sketch of installation.

in the top portion of the pipe knee is filled mainly with water vapour. In the bottom portion of the pipe water still flows for a while in the forward direction (see detail A in Fig. 1).

After the cavity has formed at A, the column AP decelerates rapidly, while the hydraulic grade line at the pump drops from E to S and eventually the check valve closes upon flow reversal through the pump. The deceleration of the column AB continues at approximately the same rate as that at the instant when water column separation starts. The hydraulic grade line DFW rises gradually to DGW and remains unchanged during the existence of the cavity. After a while the column AB comes momentarily to a stop, while the cavity reaches its maximum volume. Thereafter the column AB reverses its motion and the cavity reduces in size. Substantial velocity in reverse can be reached by the column AB before the cavity collapses. The sudden pressure head rise, at the instant of cavity collapse at A, is equal to  $(a/2g)\Delta V$ .

The collapse of the cavity causes two pressure wave fronts to form in the pipeline, one travelling upstream and the other downstream from point A. The maximum pressure head rise  $\Delta H_{\max}$  usually occurs at the pump end when the upstream travelling wave front is reflected from the closed check valve. However, these events can be further complicated by the closure of the check valve itself, which causes its own pressure wave to be superimposed on the waves resulting from the cavity collapse. If the reflection of the upstream travelling wave front coincides with the check valve closure, a pressure peak of even greater magnitude can occur.

In the past, semigraphical procedures (Bergeron 1961; Gandenberger 1950) were used to determine pressure rises resulting from water column separation. More recently, computerized techniques (Wylie and Streeter 1983; Chaudhry 1979) have been developed and attempts have been made to allow for the presence of air during water column separation.

Distributed air bubbles in the initial steady state as well as air release during the existence of cavity can substantially reduce the pressure peak caused by the joining water columns at the instant of cavity collapse. This reduction is, however, not assured. First, the air content in the pipeline cannot yet be reliably predicted. In addition, during an extended shutdown air bubbles rise to the crown and coalesce there into air pockets, which travel along the pipeline and collect at the summits if air release valves are not provided. The major part of the cushioning effect of the distributed air bubbles is therefore lost; indeed, the air pockets at the summits can now substantially increase the transient effects. Present design practice is to prevent the existence of air pockets by installing air release valves at the summits. Similarly, the effect of the air release into the cavity can vary widely. When the cavity extends over a considerable length of pipeline, the active water and vapour pocket interface becomes substantial. When such a condition occurs, a major amount of air release could result. However, a very localized high point in a line with short cavity duration could yield only a minor air release. In view of these uncertainties, it is advisable to ignore any reduction of the pressure peak caused by either distributed air bubbles or air release until more is

known about their existence and behaviour.

In this paper a systematic study is presented combining the effects of water column separation and check valve closure on the maximum pressure head rise, both initiated by power failure.

**Main parameters**

The main parameters of the pipeline are given below in classical nondimensional form (Allievi 1925). The pipeline constant

$$[1] \quad \rho = aV_0/2gH_r$$

in which  $a$  = water hammer wave velocity,  $V_0$  = initial steady state velocity in the pipe,  $g$  = acceleration of gravity, and  $H_r$  = rated pumping head.  $H_r = H_0 + H_f + H_l + H_v$ , where  $H_0$  = static head,  $H_f$  = head loss due to pipe wall friction and viscosity in the initial steady state,  $H_l$  = sum of local losses (check valve, gate valve, pump header junction, etc.), and  $H_v$  = velocity head in initial steady state.

The pipe wall friction, local losses, and velocity head are lumped together and considered in the non-dimensional form

$$[2] \quad h_r = \frac{H_f + H_l + H_v}{H_r}$$

in which friction  $H_f = f(L/D) (V_0^2/2g)$  by Darcy-Weisbach, where  $f$  = friction factor,  $L$  = length of pipe,  $D$  = pipe diameter, local loss  $H_l = KV_0^2/2g$ , where  $K$  = local loss coefficient, velocity head  $H_v = V_0^2/2g$ , and  $h_r$  = total relative head loss.

The pump constant is

$$[3] \quad K_1 = \left(\frac{60}{2\pi}\right)^2 \frac{gwH_rQ_r}{WR^2\eta_rN_r^2}$$

to be used in the equation of angular deceleration

$$[4] \quad \Delta\alpha = K_1\beta_a\Delta t$$

in which  $w$  = unit weight of water,  $Q_r$  = rated discharge through one pump,  $WR^2$  = moment of inertia of rotating parts of one unit including water in the impeller,  $\eta_r$  = pump efficiency at the rated condition,  $N_r$  = rated pump speed,  $\Delta\alpha = (N_1 - N_2)/N_r$  is the non-dimensional speed reduction during a small time interval  $\Delta t$ ,  $N_1$  and  $N_2$  = transient pump speeds at the beginning and at the end of the time interval  $\Delta t$ , and  $\beta_a$  = average relative torque.

The nondimensional time is

$$[5] \quad t' = t/\mu$$

in which  $t$  = time in seconds and  $\mu = 2L/a$  is the time constant.

The pump constant  $K_1$  and the time constant  $\mu$  can be conveniently combined into a single dimensionless

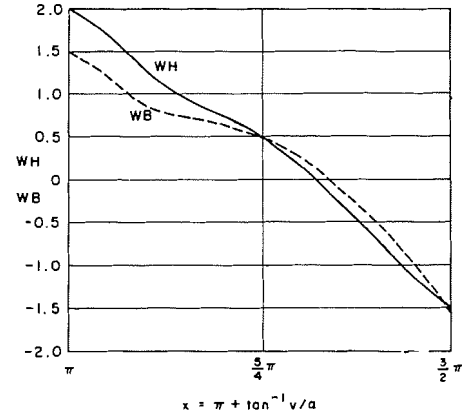


FIG. 2. Pump characteristics, normal pump operation.

ratio

$$[6] \quad \tau = \frac{1}{K_1\mu}$$

The complete characteristics of a pump (Donsky 1961; Wylie and Streeter 1983) with a specific speed  $N_s = 147$  (7600) rpm are used in the zone of normal pump operation (see Fig. 2).

To adapt the pump characteristics for computer use, the dimensionless ratios

$$[7] \quad h = \frac{H}{H_r} \quad \beta = \frac{T}{T_r} \quad v = \frac{Q}{Q_r} \quad \alpha = \frac{N}{N_r}$$

are employed. In these ratios  $H$ ,  $T$ ,  $Q$ , and  $N$  are the transient head, torque, discharge, and speed. The subscript  $r$  indicates these quantities at the rated condition. With the dimensionless ratios for homologous pumps, and with the transformation proposed by Marshal *et al.* (1965), the expressions

$$[8] \quad WH(x) = \frac{h}{\alpha^2 + v^2} \quad WB(x) = \frac{\beta}{\alpha^2 + v^2} \quad x = \pi + \tan^{-1} \frac{v}{\alpha}$$

are obtained for the relative head  $WH$  and the torque  $WB$ . The data are available in tabular form (Wylie and Streeter 1983) for equal intervals of  $x = \pi/44$  rad, and are used to plot the characteristics shown in Fig. 2.

The relative horizontal location of the high point  $A$  in Fig. 1 is designated by

$$[9] \quad r_1 = X/L$$

in which  $X$  = distance from the pump end, measured along the pipe.

The relative elevation of the high point is designated by

$$[10] \quad r_2 = Y/H_r$$

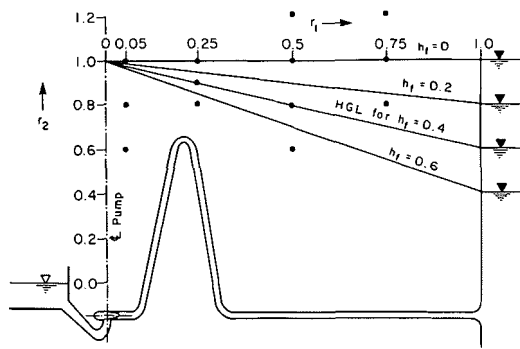


FIG. 3. Sketch of high point location.

in which  $Y$  = vertical distance from the elevation of water surface in the sump to the elevation of the high point (see Figs. 1 and 3).

### Basic assumptions

In the analyses, it is assumed that (a) the pipe diameter and wall thickness are constant, (b) the check valve is located near the pump, (c) the closure of check valve occurs suddenly at the instant of flow reversal through the pump, (d) only one localized high point exists (see Fig. 3) in which water column separation occurs, (e) no dispersed air bubbles exist in the initial steady state, no air pocket exists in the high point prior to or during water column separation, and no air release occurs in the cavity during water column separation, (f) the velocity head and local losses are lumped together with pipe wall friction, (g) the difference between the atmospheric pressure head and the vapour pressure head is equal to 9.6 m (31.50 ft), e.g. water column separation starts at a pressure head of  $-9.6$  m, (h) the suction piping is short and can be disregarded, (i) the pump is working in the rated condition in the initial steady state, i.e. at the point of best efficiency.

### Calculations and results

Two partial differential equations describing the unsteady flow are transformed into four total differential equations by the method of characteristics. Two separate computer programs are written to solve these total differential equations with appropriate boundary conditions for the range of  $\rho$ ,  $\tau$ , and  $h_f$  normally encountered in pumping systems using the approach of specified time intervals (Wylie and Streeter 1983). In the calculations for the maximum pressure head rise, the pipe is usually divided into 40 equal reaches of  $\Delta x$ . In cases where no column separation occurs, runs with 20 reaches are made. A time interval  $\Delta t = \Delta x/a$  is used throughout the calculations.

For each separate combination of  $r_1$ ,  $r_2$ ,  $h_f$ ,  $\rho$ , and  $\tau$  one maximum pressure head rise is calculated. This

maximum, which usually occurs at the pump end, must be considered for the entire pipeline.

The first of the two programs analyzes the basic system consisting of the pump, the check valve, the pipe, and the reservoir for a power failure condition with the check valve closing upon the flow reversal through the pump. No high point exists and no water column separation is considered.

This program calculates firstly the maximum downsurge at the pump end, at the midpoint, and at the three-quarter point near the reservoir. The results are shown in Figs. 4–6, which give the downsurge in terms of the rated pumping head  $H_r$  on the  $\tau$ – $\rho$  plane for various pipe friction values  $h_f$  at these locations. Separate curves are drawn in these figures for  $h_f = 0.0, 0.2, 0.4,$  and  $0.6$ . Intermediate values of pipe wall friction can be considered by interpolating between the curves. The curves are only slightly smoothed computer plots. The numbers on the curves indicate the maximum relative pressure head drop and are measured downward from the initial steady state pressure head at the pump.

Using the plotted values of maximum pressure head drop at the pump end, midpoint, and three-quarter point along with the value at the reservoir end, which has a pressure head drop of zero, an enveloping curve can be drawn. This curve will show the maximum pressure head drop along the entire pipeline. This curve, when plotted on the profile of the pipeline, will enable the designer to see in one glance, and with good accuracy, whether or not water column separation is expected at any point along the pipeline.

Secondly this program calculates the maximum upsurge at the pump end. The results are shown in Fig. 7, which gives the maximum pressure head rise in terms of the pumping head  $H_r$ . The numbers on the curves indicate the maximum relative pressure head rise and are measured upward from the initial steady state pressure head at the pump. In this case the smoothed computer plots are quite accurately shown as straight lines. The maximum relative pressure head rise at the pump approaches 1.0 for low  $\tau$  and high  $\rho$  values for the case of frictionless flow. For cases of large friction, this rise is drastically reduced.

The results for frictionless flow were compared at the pump end and at the mid-length with those reported by Donsky (1961), obtained using the same pump characteristics and the graphical method of water hammer analysis. Very good agreement was observed at both downsurge and upsurge conditions. Because of the slow and gradual variation of the maximum pressure head rise obtained from this program, only a limited number of points needs to be calculated.

The second program includes the analysis of water column separation, which occurs in the high point. This program is identical with the first one in all other re-

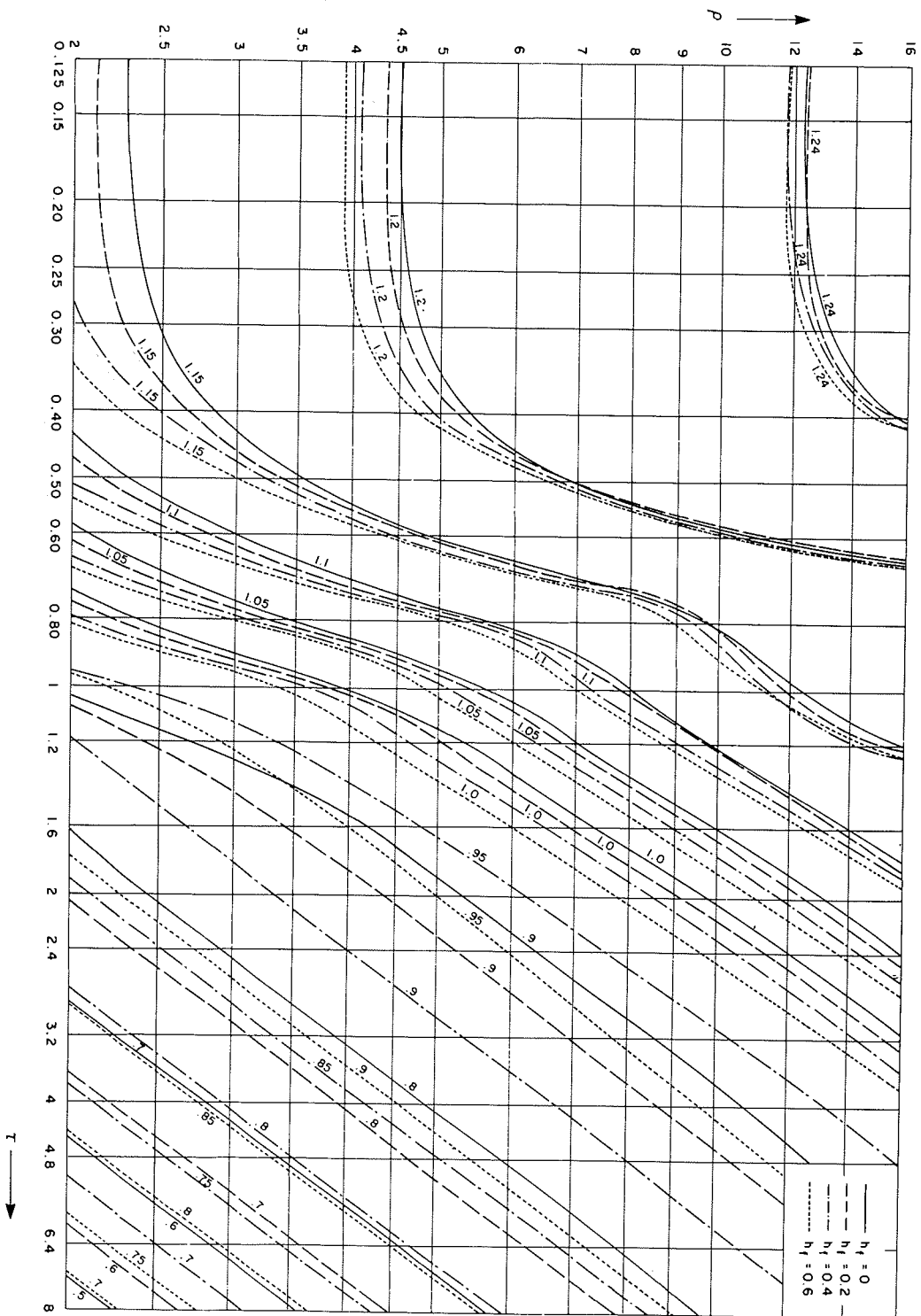


FIG. 4. Maximum downsurge at pump end, no column separation.

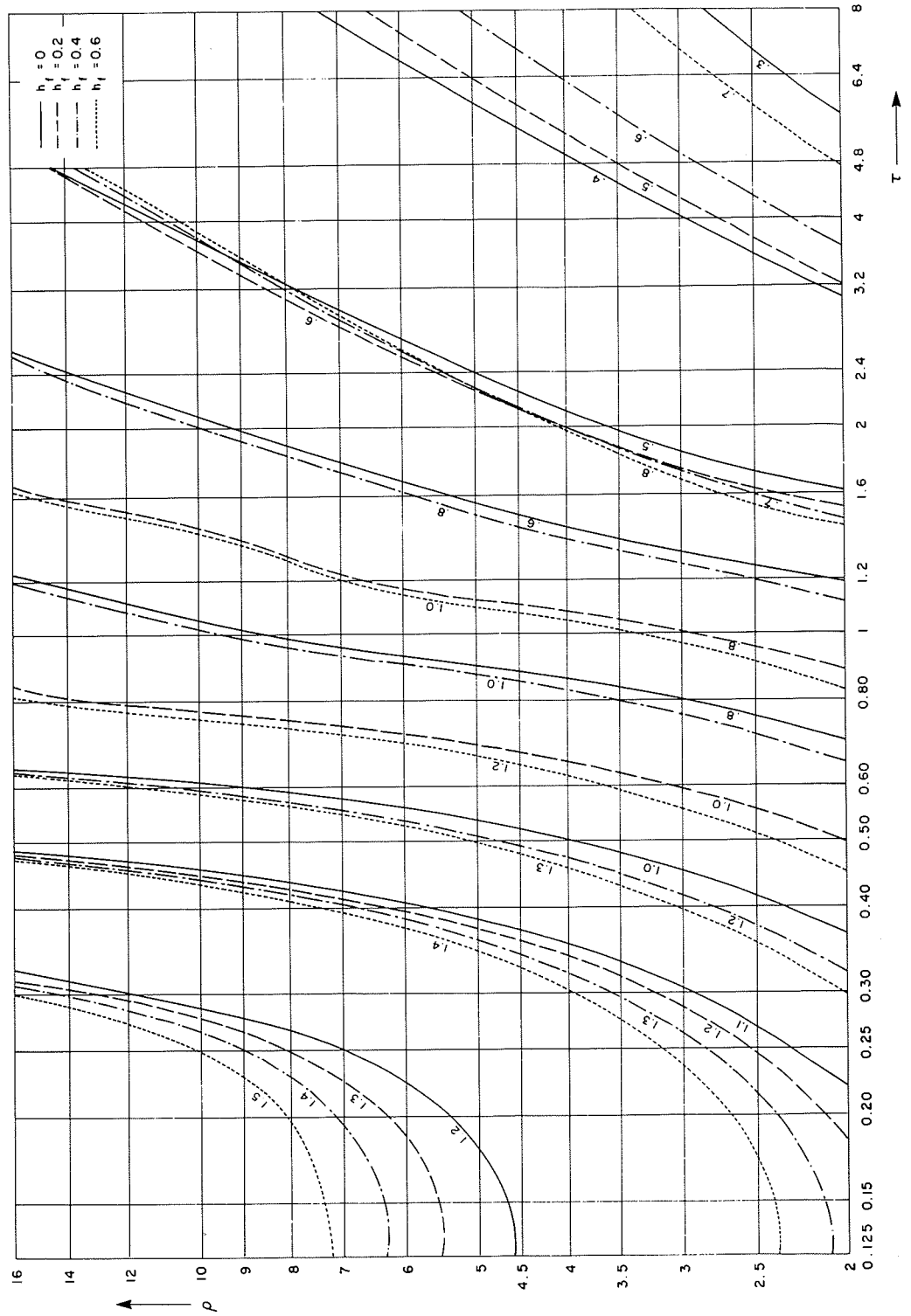


FIG. 5. Maximum downsurge at midpoint, no column separation.

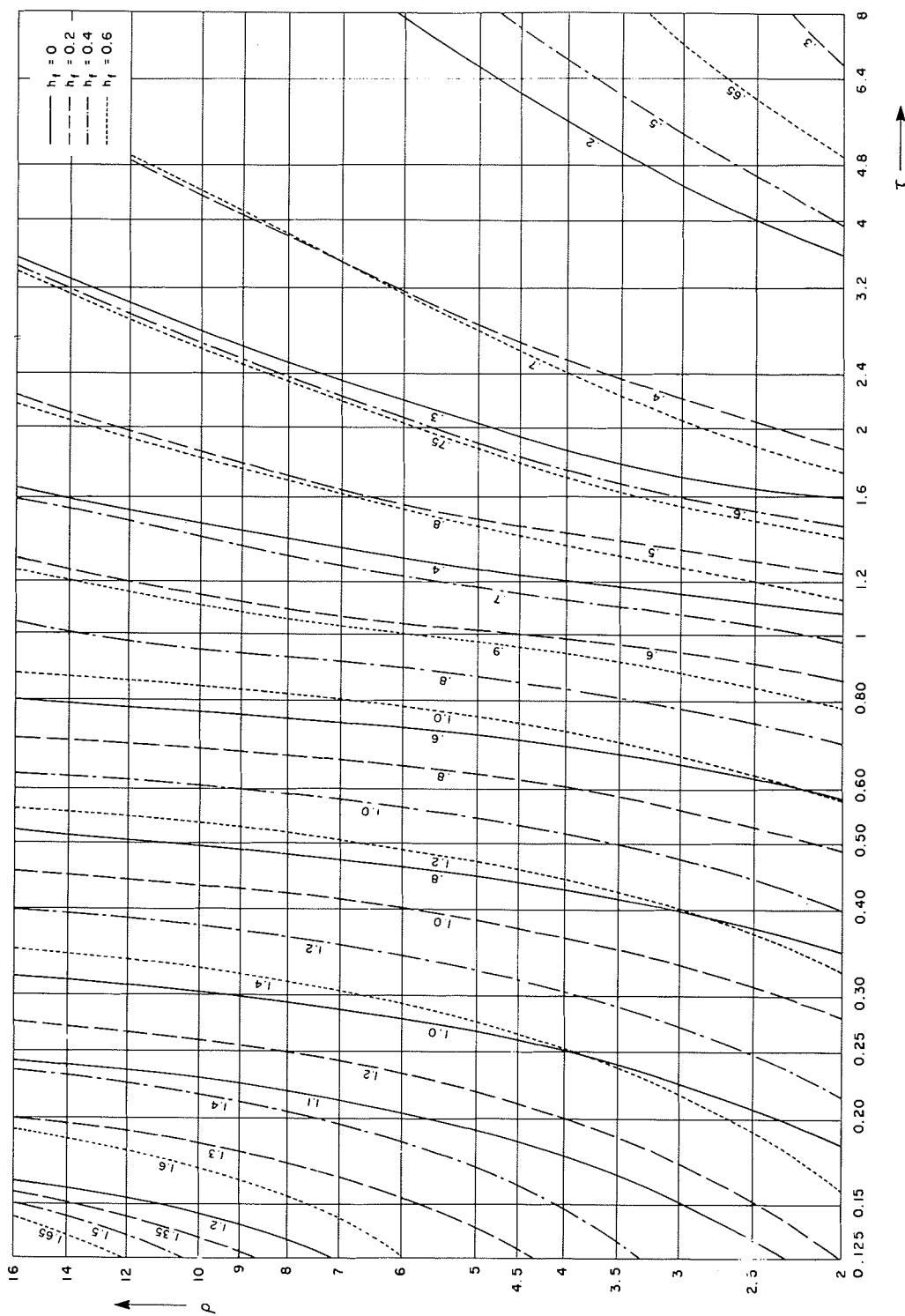


FIG. 6. Maximum downsurge at three-quarter point, no column separation.

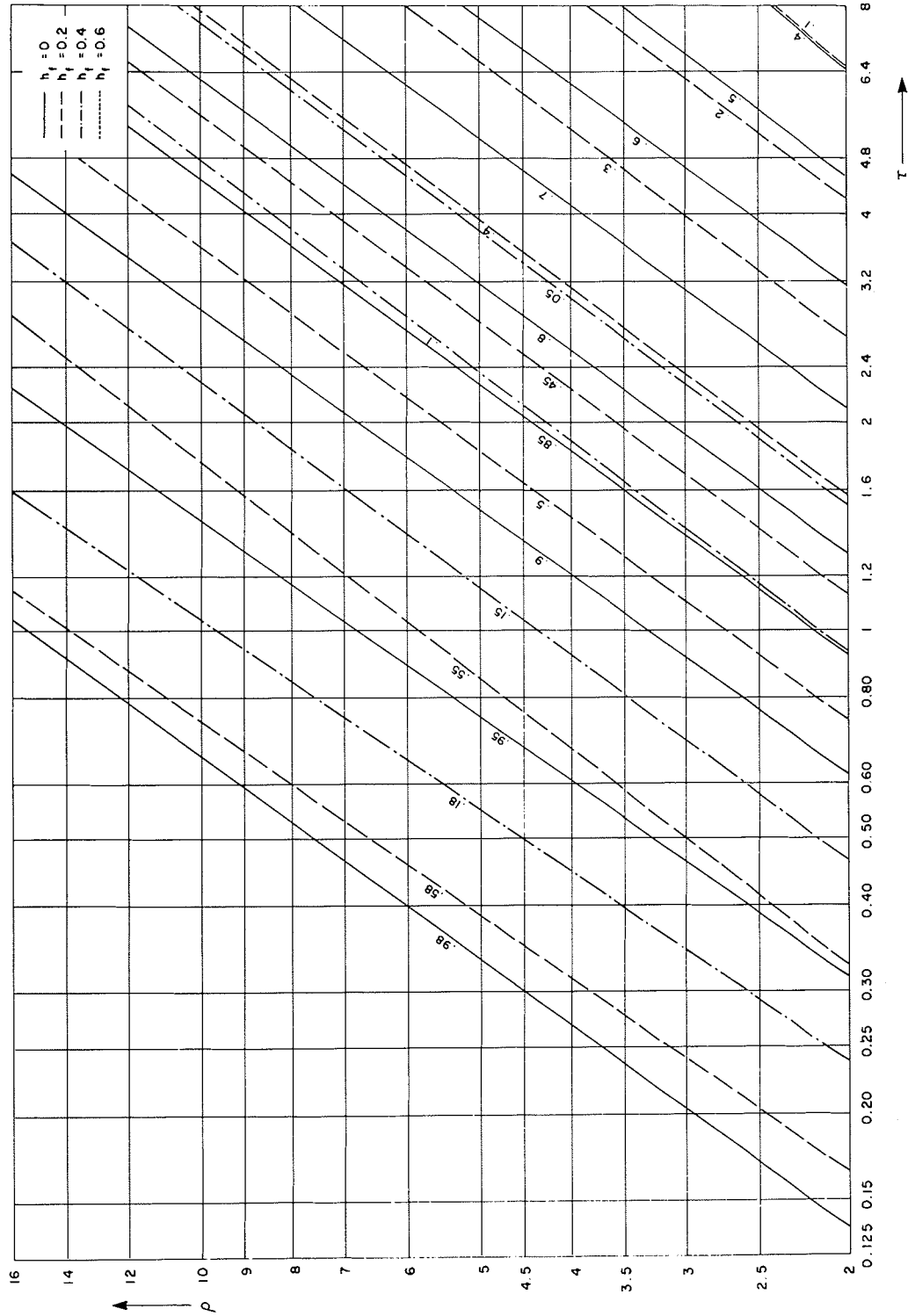


FIG. 7. Maximum upsurge at pump end, no column separation.

spects. In the second program, each of the relative values of pipe friction  $h_f = 0.0, 0.2, 0.4,$  and  $0.6$  is considered together with up to 97 values of the pipeline constant  $\rho$  ranging from 2.0 to 16.0 and with 33 values of the inertia parameter  $\tau$  ranging from 0.125 to 2.0. Over 10 000 extreme pressure rises are calculated for each of the 13 high points considered (Fig. 3). The results of the second program are superimposed on those of the first program and presented as curves of equal maximum pressure head rise on the double logarithmic graphs in Figs. 8–20. In this way the pressure head increase due to water column separation can be easily identified.

The curves shown in these figures are hand-drawn enveloping curves based on the computer plots. A sample of the computer plot with the corresponding hand-drawn enveloping curves for a case including column separation is shown in Fig. 21.

The graphs in Figs. 8–20 have been derived for a total pumping head  $H_r$  and a barometric pressure head  $H_b$  equal to 12 m (39.37 ft) and 9.6 m (31.50 ft) respectively. The numbers on the curves indicate the maximum relative pressure head rise in terms of this pumping head and are measured upward from this initial steady state pressure head at the pump.

In pipelines with large friction ( $h_f > 0.4$ ), the upsurge may never reach the initial steady state pressure head at the pump. In such cases a zero pressure head rise is indicated on the graphs.

A large-scale analysis of water column separation, using the data of the same pump and the graphical method of water hammer analysis was carried out by the writers to spot check the validity of the results obtained by the computer program. Very good agreement was obtained.

### Discussion of results

Smooth and gradual variation in the maximum pressure head drop and rise at the pump end is noticed on the double logarithmic plot in the studied range of variables  $\rho$ ,  $\tau$  and,  $h_f$  when no water column separation occurs (see Figs. 4–7). On the other hand, large local pressure head changes can occur whenever water column separation is present. The largest pressure rises in such cases usually occur at high  $\rho$  values combined with low  $\tau$  values. Large deviations, however, appear in this general pattern, depending on the horizontal location and the elevation of the high point and on pipe friction. Little or no water column separation is experienced when low  $\rho$  values are combined with high  $\tau$  values. The check valve closure at the instant of flow reversal determines the maximum pressure head rise in the latter cases.

With the graphs presented in this paper, one can easily see which combinations of  $\rho$ ,  $\tau$ , and  $h_f$  lead to

water column separation in a given high point and what is the resulting pressure head rise. The graphs also give a clear indication of how to change  $\rho$  and  $\tau$  to avoid column separation.

The maximum pressure head change depends largely on the pipe friction. Linear interpolation for friction is sufficient in many cases, but parabolic interpolation should be used for the regions of rapid pressure head variations. Parabolic interpolations in the vertical and horizontal direction are also needed when considering high point locations other than the ones examined in the paper.

The graphs give the pressure head rises quite accurately for the basic data used in the analyses. However, one must bear in mind that  $\rho$ ,  $\tau$ , and  $h_f$  values are usually not accurately known in field conditions. In addition, the characteristics of the pump may be substantially different from those used in derivation of the graphs because of different specific speed<sup>1</sup> and different design of the pump. Moreover the double interpolation required for the high point (in the vertical and horizontal direction) and the interpolation required for friction introduces additional inaccuracies. Therefore a margin for possible variation for variables  $\rho$ ,  $\tau$  and  $h_f$  must be allowed, particularly in areas where large pressure peaks occur. For both  $\rho$  and  $\tau$  values a margin of at least  $\pm 10\%$  is suggested.

The graphs, in particular those with  $r_1 = 0.75$  and  $r_1 = 0.50$ , show that the largest  $\rho$  value (corresponding to the maximum velocity) does not necessarily result in the maximum pressure head rise. A  $\rho$  value substantially less than  $\rho_{\max} \pm 10\%$  could be critical, and therefore partial flows must be considered whenever such flows can occur for any considerable duration of pump operation. When doing this, the change in  $K_1$ , caused by changes in  $Q_r$ ,  $H_r$ , and  $\eta_r$ , needs to be considered. Pipe friction  $h_f$  will also change for reduced flows and some consideration should be given to the loss of the valve at the outlet (if present).

The graphs are intended primarily for the preliminary design for large pipelines having only one well-defined high point, where only a localized column separation occurs. The graphs should be sufficient for final design of small pipelines, if an ample margin is applied. A computer program should be used to analyze a pipeline with two or more high points and in cases where the cavitating flow extends over a substantial length of pipe. Such programs should include some consideration of air release.

<sup>1</sup>According to Kinno and Kennedy (Kinno and Kennedy 1965) the pressure drop in the downsurge condition is rather insensitive to the specific speed and design of the pump. Therefore only a small inaccuracy is expected in downsurge because of these reasons.

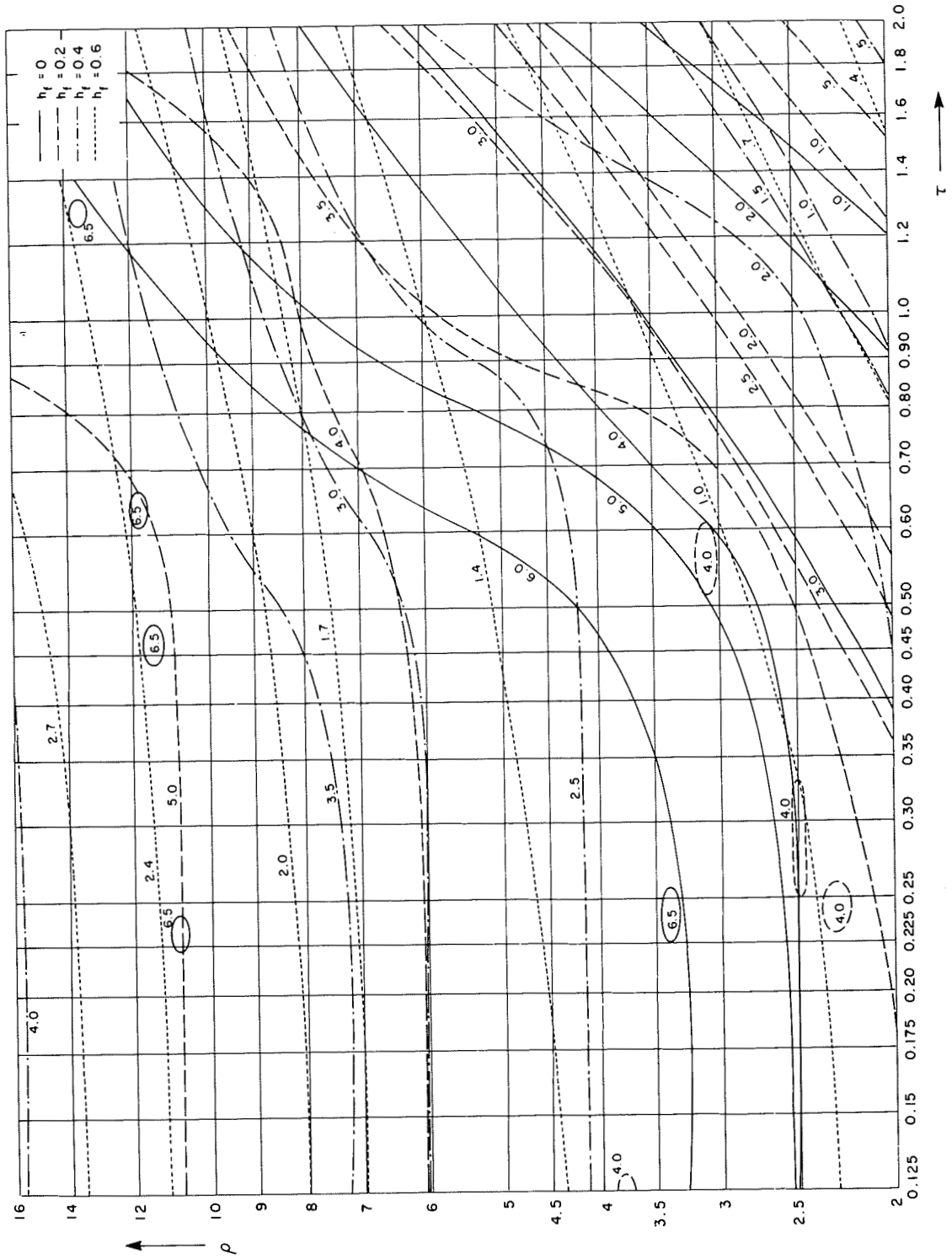


FIG. 8. Maximum upsurge  $r_1 = 0.05$ ,  $r_2 = 1.00$ .

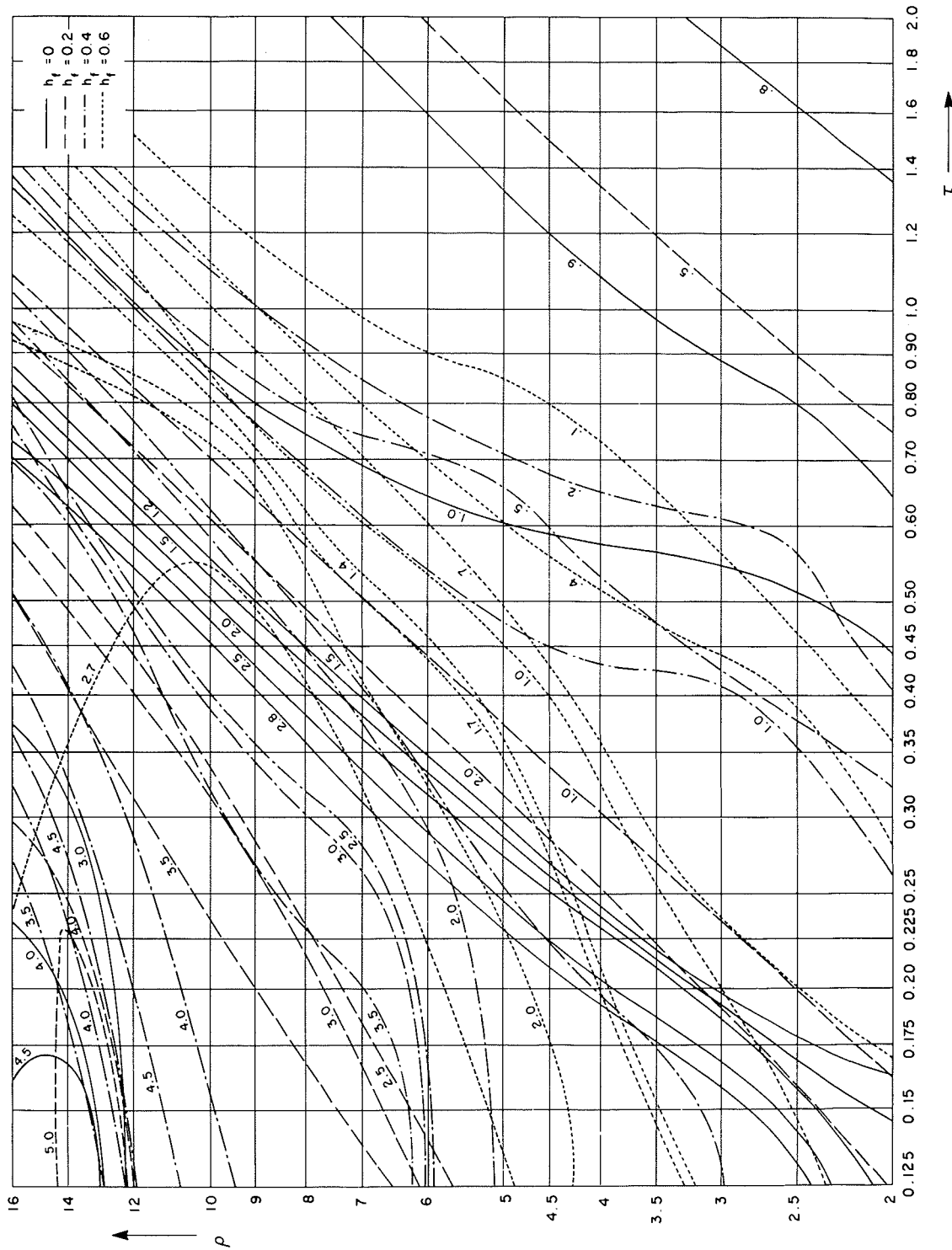


FIG. 9. Maximum surge  $r_1 = 0.05, r_2 = 0.80$ .

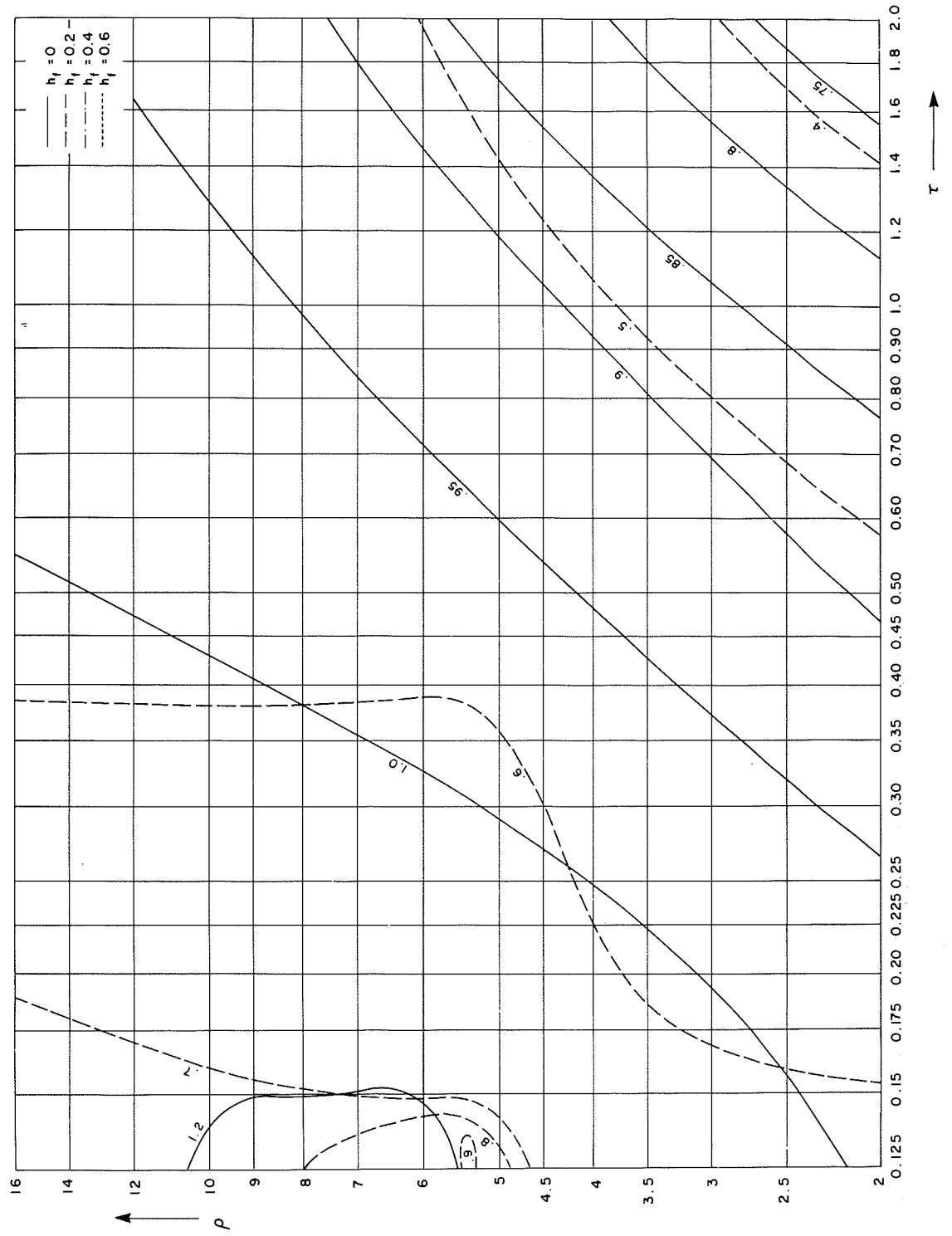


FIG. 10. Maximum upsurge  $r_1 = 0.05$ ,  $r_2 = 0.60$ .

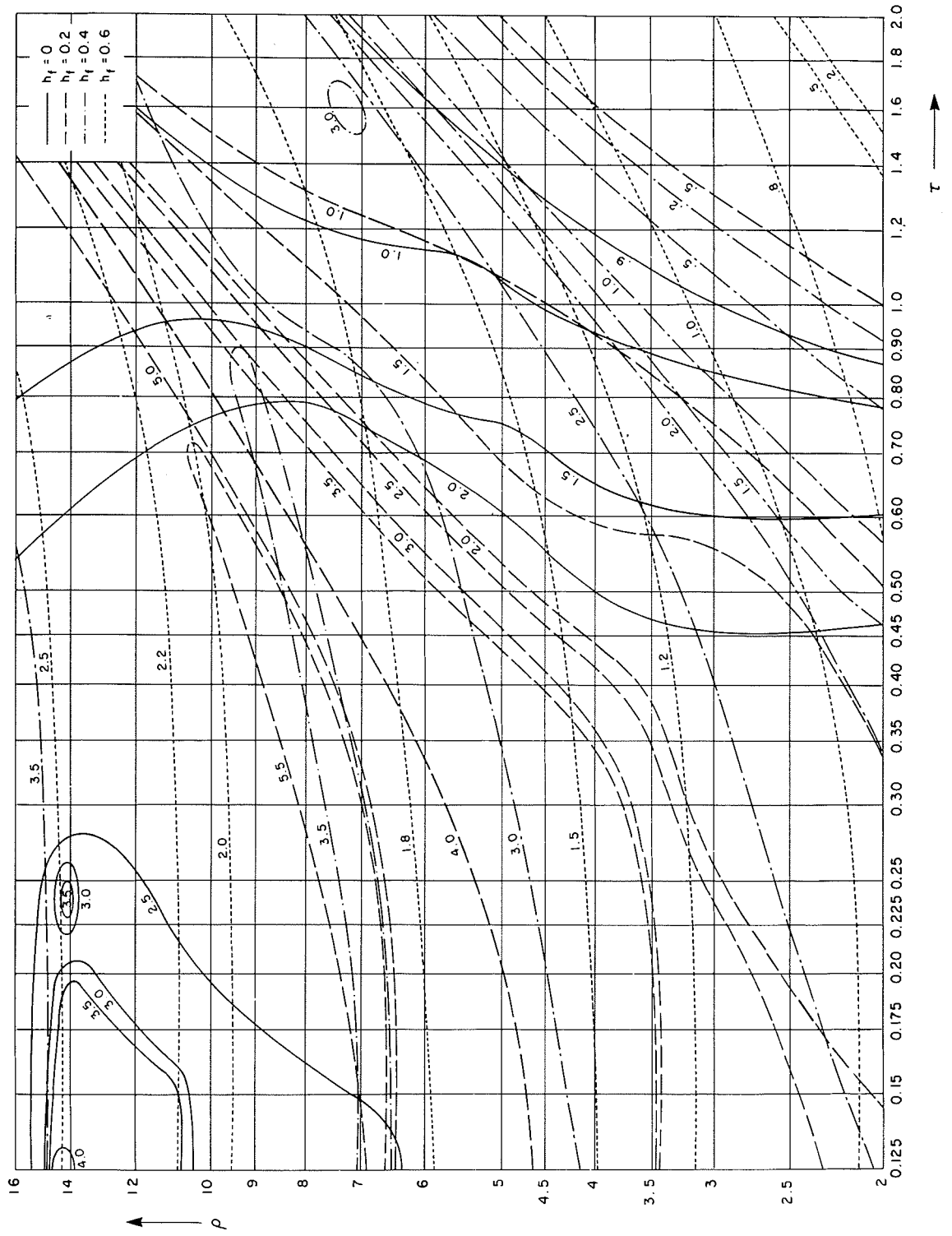


FIG. 11. Maximum upsurge  $r_1 = 0.25$ ,  $r_2 = 1.00$ .

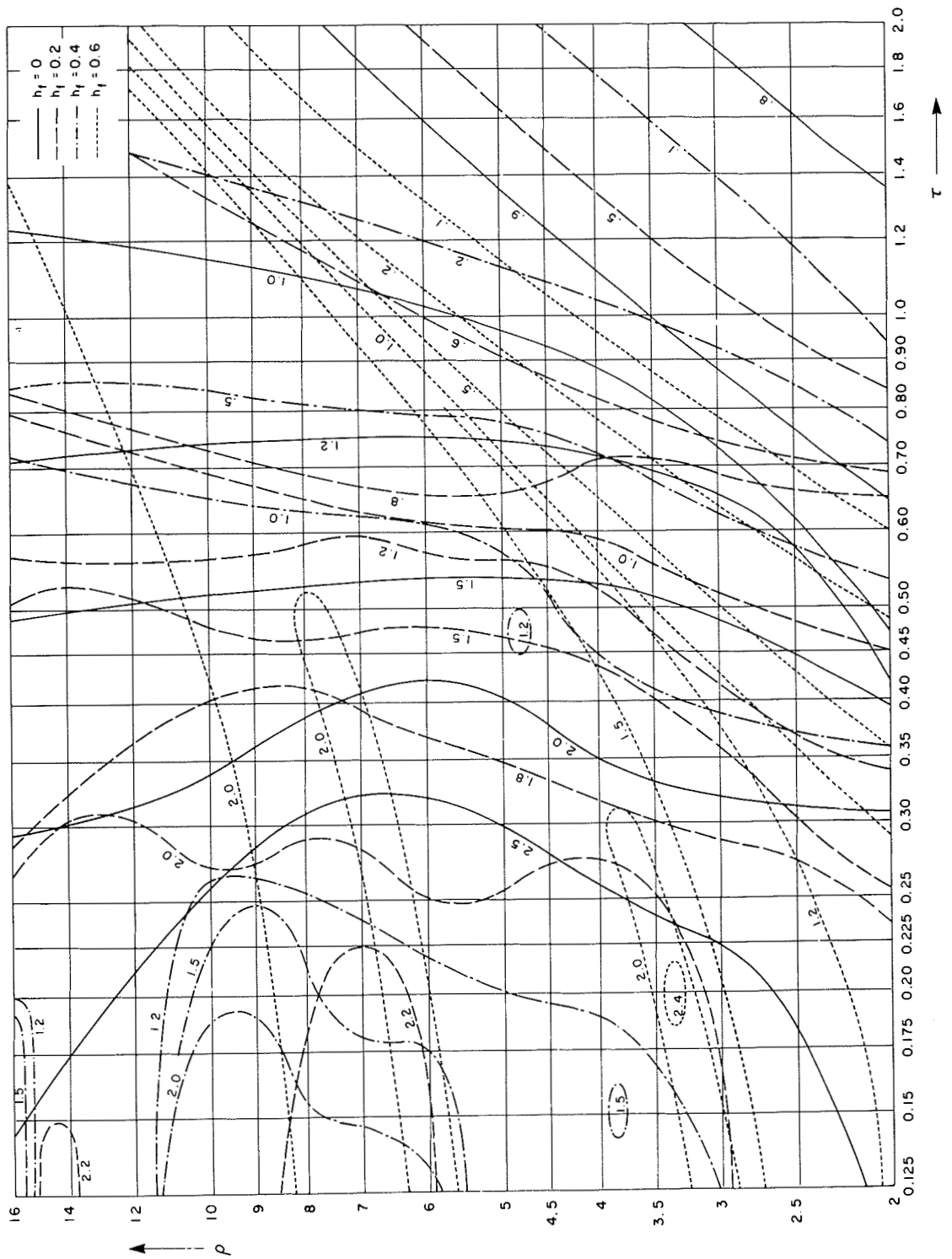


FIG. 12. Maximum upsurge  $r_1 = 0.25$ ,  $r_2 = 0.90$ .



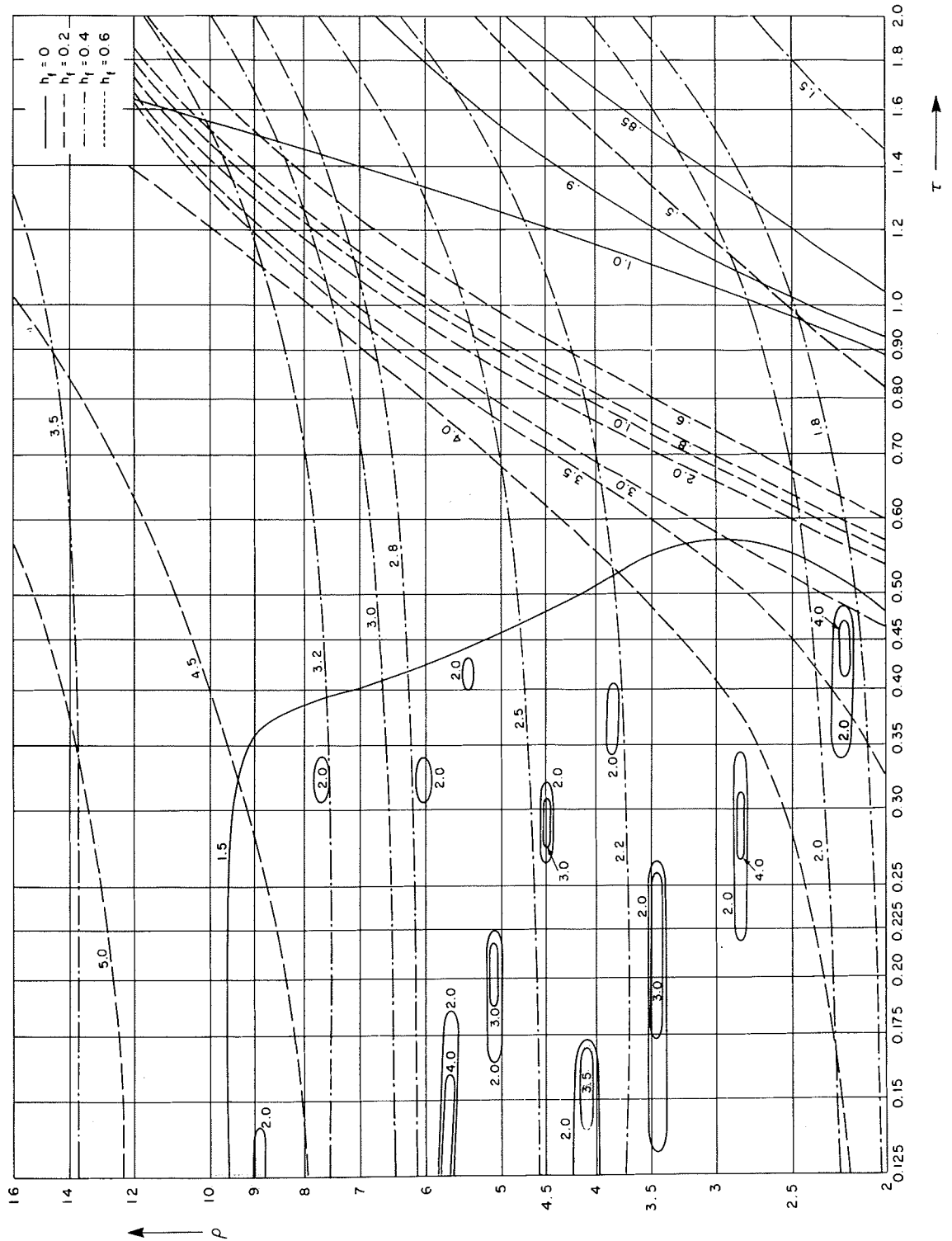


FIG. 14. Maximum upsurge  $r_1 = 0.50, r_2 = 1.20$ .

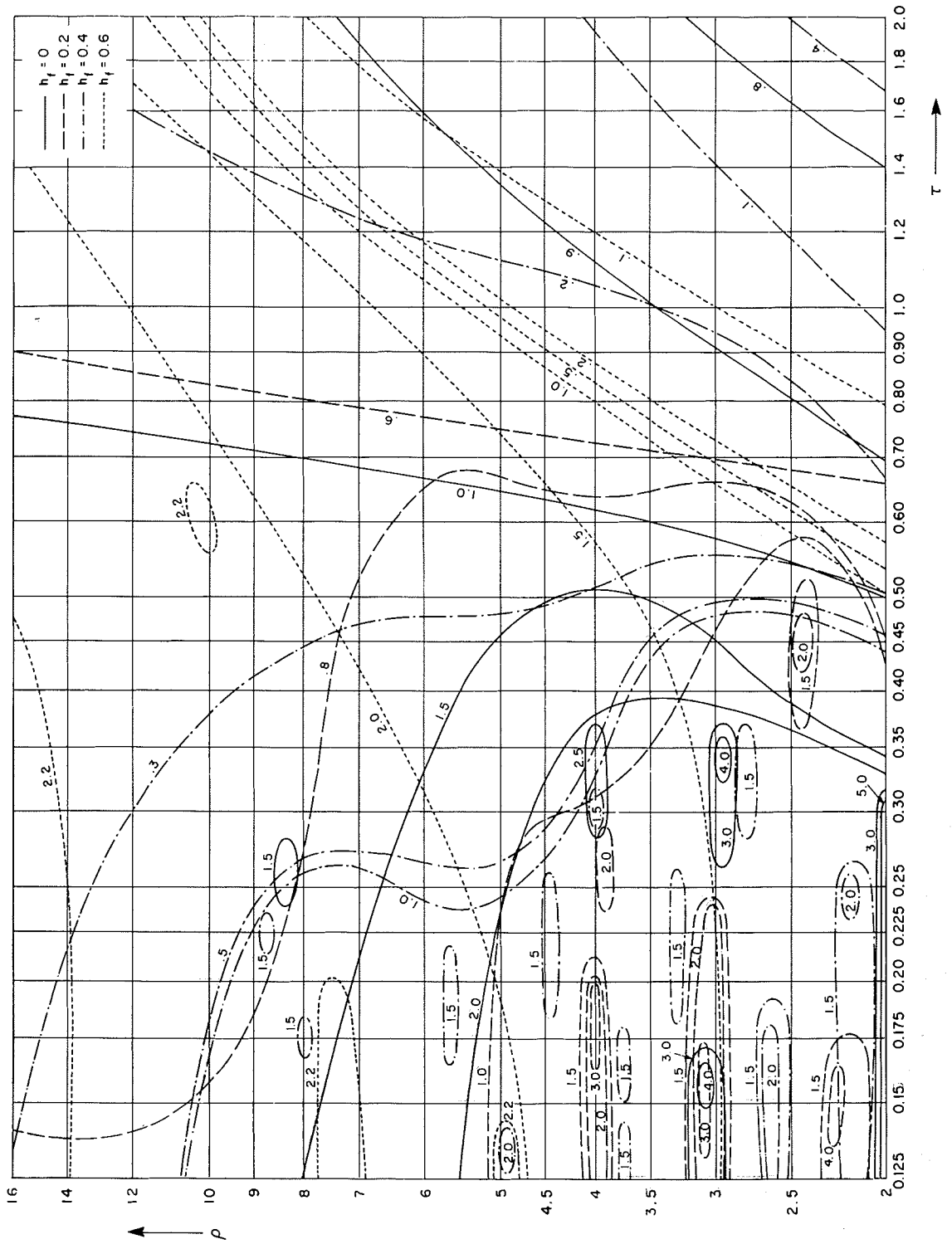


FIG. 15. Maximum upsurge  $r_1 = 0.50, r_2 = 1.00$ .

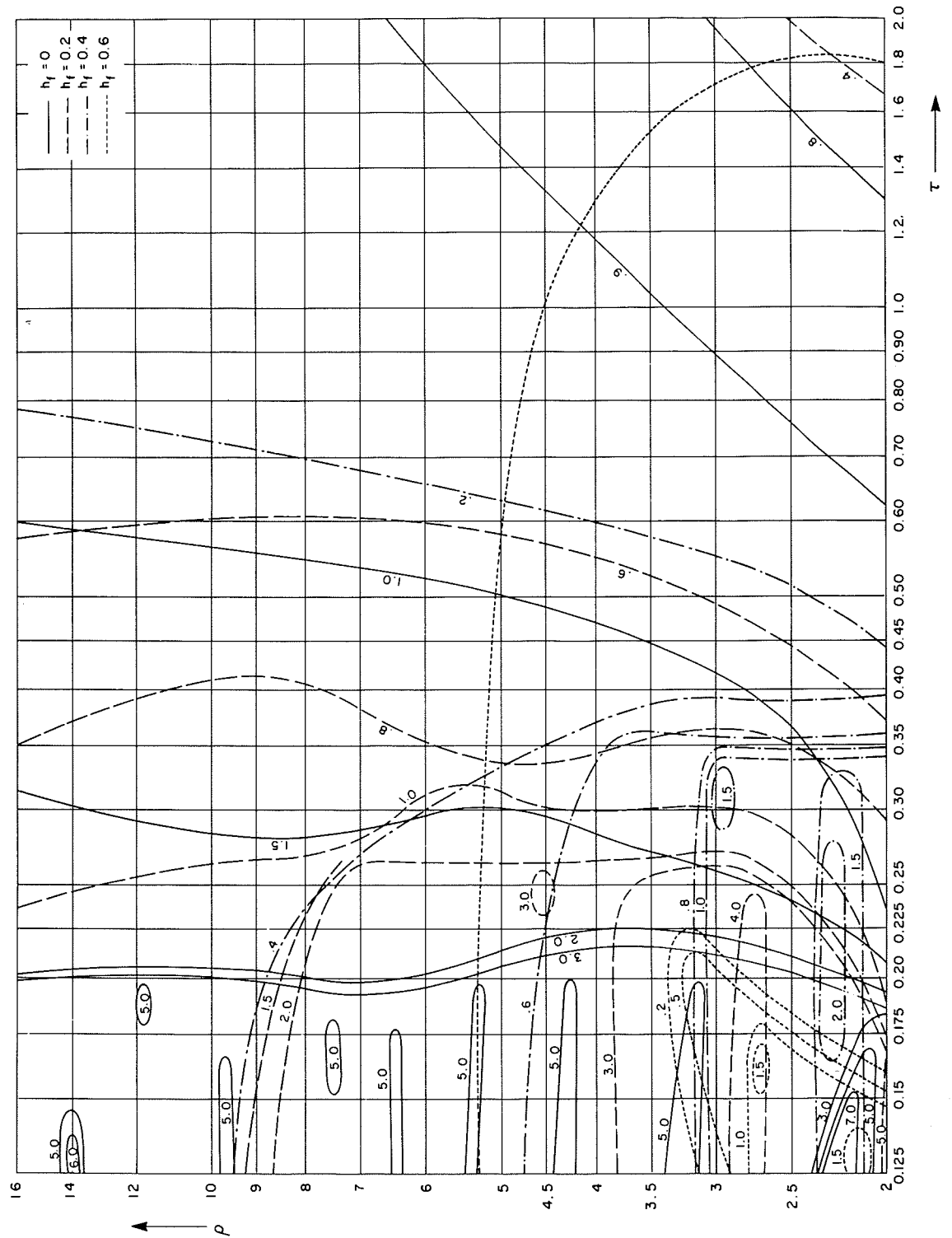


Fig. 16. Maximum upsurge  $r_1 = 0.50, r_2 = 0.80$ .



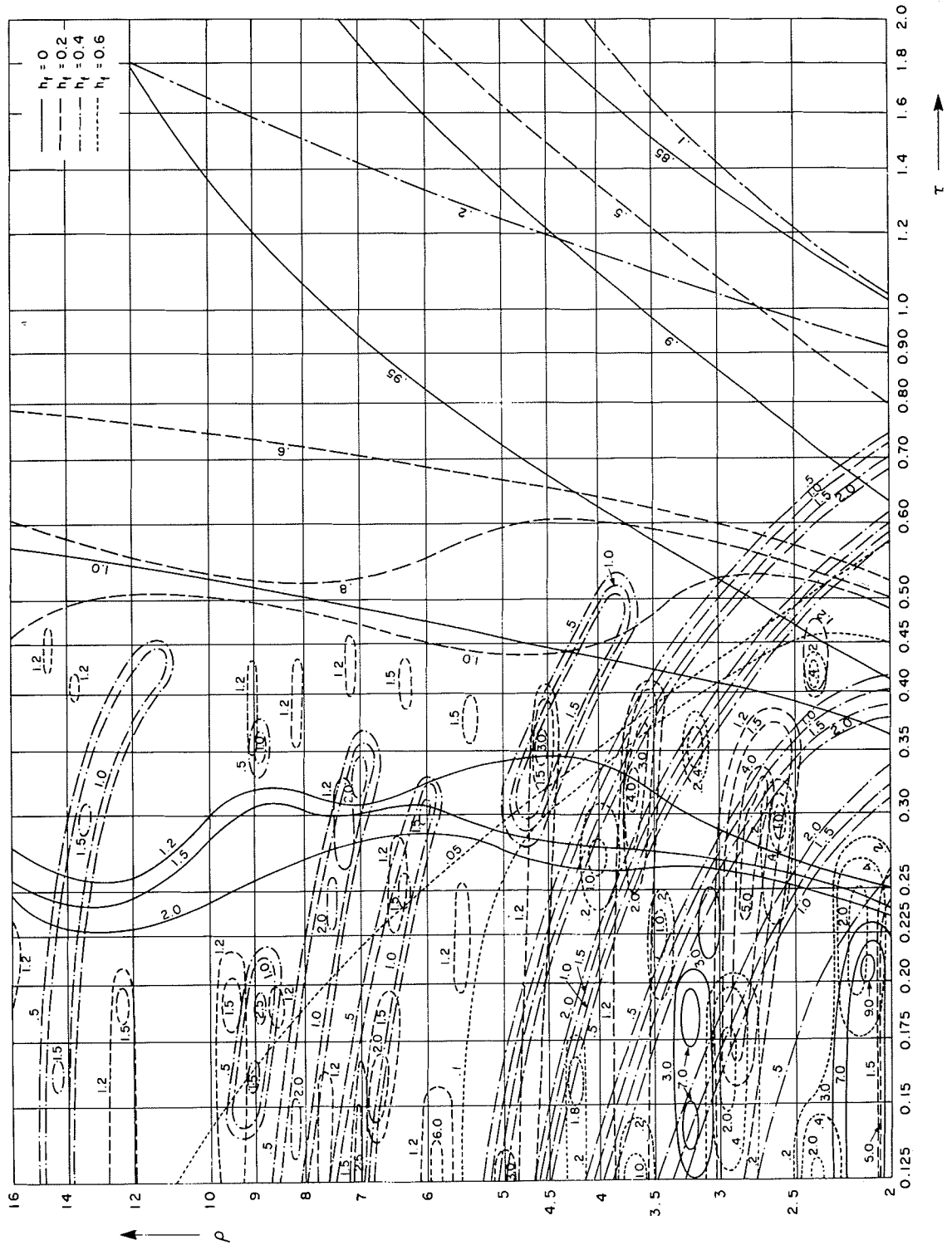


FIG. 18. Maximum upsurge  $r_1 = 0.75$ ,  $r_2 = 1.20$ .

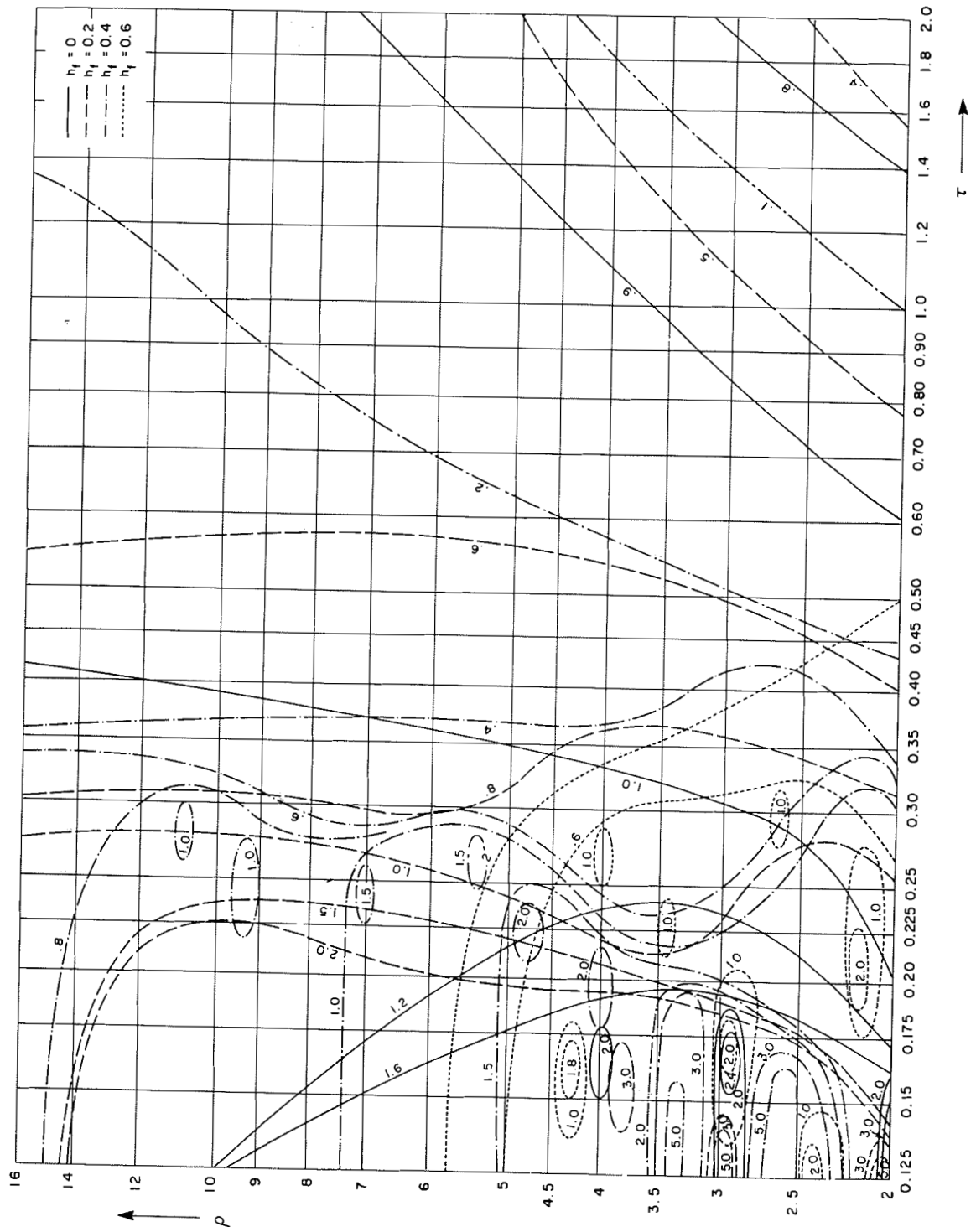


FIG. 19. Maximum upsurge  $r_1 = 0.75$ ,  $r_2 = 1.00$ .

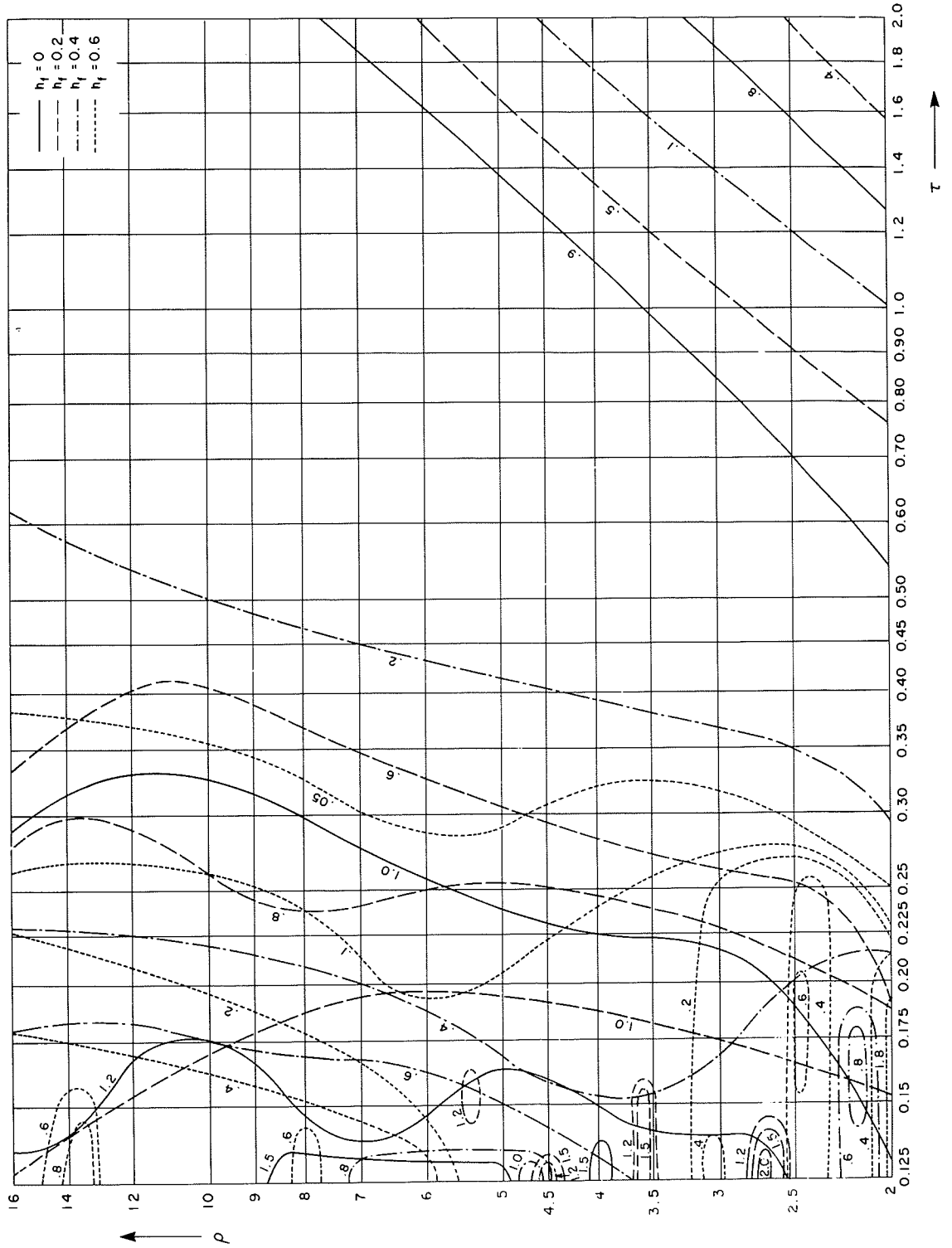


Fig. 20. Maximum upsurge  $r_1 = 0.75, r_2 = 0.80$ .

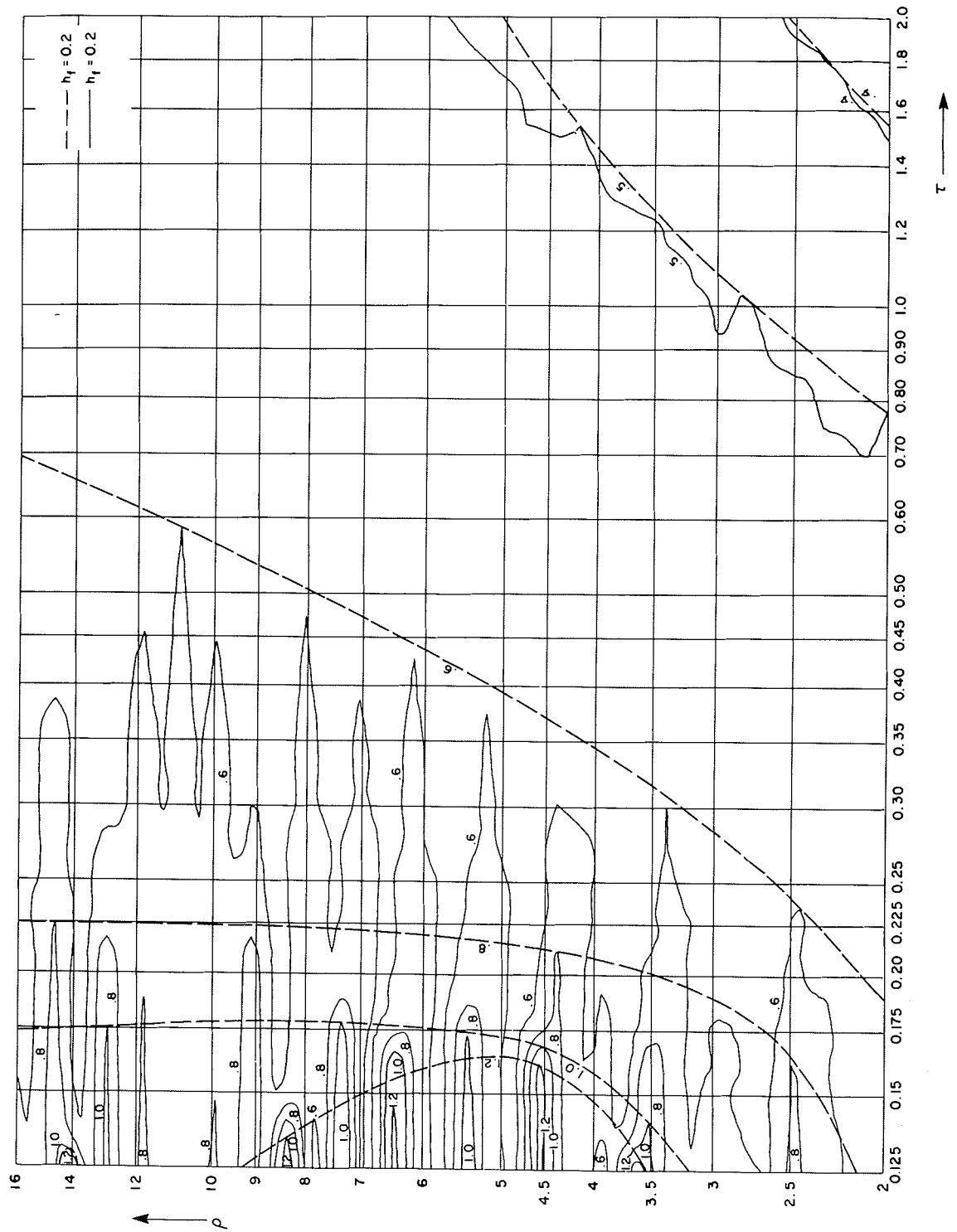


FIG. 21. Example of computer plot.

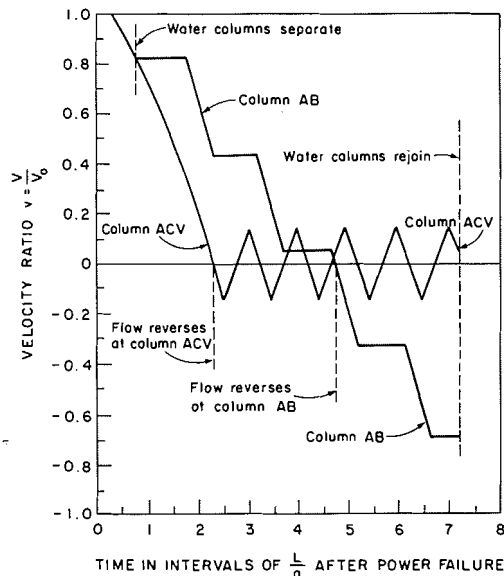


FIG. 22. Velocities of upstream and downstream water columns after separation.

### Pressure head peaks

When no water column separation occurs, the variation in pressure head rise is fairly smooth and gradual in both directions on the  $\tau$  and  $\rho$  plane (see Figs. 4–7). Whenever water column separation does occur, the whole area on computer plot that is influenced by water column separation is covered by individual, more or less sharp pressure head peaks, separated by valleys of lower pressure head rise. Most of these peaks are much sharper and more pronounced than those shown in Fig. 21. These pressure peaks are usually represented by enveloping curves in a fashion indicated in Fig. 21.

The distribution of the peaks is rather complex. Depending on the location of the high point, many individual pressure head peaks appear in groups, which are oriented as straight lines predominantly in the direction of the  $\tau$ - $\rho$  axis. For a given  $\tau$  value, there can be up to 16 distinct pressure head peaks. Figure 18 shows most of these peaks for  $h_f = 0.2$ . A few of the groups are oriented in some intermediate direction, and for the highest point investigated at three-quarter length of pipe with  $h_f = 0.4$ , the pressure peaks are lying on a curve (Fig. 18). In numerous cases, pressure peaks also occur at random.

The computer plots indicate clearly that friction has a large effect on the location and magnitude of the pressure head peaks. In general, a relative friction  $h_f = 0.2$  results in highest pressure head rises. The pressure head peaks shown in Figs. 8–20 are indicated individually where these are pronounced and located far apart on the computer plot; enveloping curves are drawn when these peaks are less pronounced and close together.

A detailed explanation for the number, location, and the orientation of the pressure head peaks is difficult to give because many variables are involved. A few general comments follow.

Figure 22 shows the typical relative velocities of the water columns during a vapour cavity. After the beginning of column separation, the velocity of the downstream water column AB reduces until the column comes to rest, then reverses its motion and reaches a substantial velocity in reverse at the instant of cavity collapse. During this time, the velocity of the water column ACV is also reduced to zero and this column continues to oscillate around zero velocity as indicated in Fig. 22. The period of this oscillation depends on the  $\tau$  value and the amplitude on the  $\rho$  value.

The immediate pressure head peak at the collapse of a vapour cavity depends on the velocity difference between the water columns on either side of the cavity. For a case where the high point is located near the reservoir end ( $r_1 = 0.75$ ), the column ACV is relatively long and therefore the vapour cavity could exist from only a fraction of the period to maybe 2–3 periods of the oscillation of column ACV. The magnitude of the oscillating velocity may reach a substantial fraction of the initial steady state velocity. Depending on the duration of vapour cavity, the rejoining of the departed water columns can occur at any velocity between the maximum and the minimum velocity of the oscillating column ACV. From Fig. 22, it appears that the maximum (positive) velocity will result in much greater immediate pressure head rise than the minimum (negative) velocity. This explains to a large extent why, for  $r_1 = 0.75$ , many sharp and pronounced pressure head peaks occur in the area influenced by water column separation on the  $\tau$ - $\rho$  plane.

In the other extreme, for cases where the high point and the water column separation occurs very near the pump ( $r_1 = 0.05$ ) the column ACV is short. Hence many velocity oscillations of short period and small amplitude occur during the existence of vapour cavity. Therefore it makes no substantial difference whether the velocity of the column ACV is positive or negative at the instant of cavity collapse. Consequently only a few less pronounced pressure head peaks occur in an undulating pressure head surface for  $r_1 = 0.05$ .

High points at the quarter length,  $r_1 = 0.25$ , and at the mid-length,  $r_1 = 0.5$ , cause more pronounced pressure head undulations. At these points, the pressure head peaks are more frequent and substantially sharper than those at  $r_1 = 0.05$ , although they are more mild than the peaks at the three-quarter length with  $r_1 = 0.75$ .

Whereas the number and the intensity of the pressure head peaks increase as the location of the high point moves in the downstream direction, the general pressure head intensity increases when the location of the

high point moves in the upstream direction.

The pressure peaks discussed above are modified by check valve closure, which is nearly independent of cavity collapse and can occur before, after, or simultaneously with a cavity collapse. Most of the pressure peaks resulted not from the first cavity collapse but from the first cavity collapse that followed check valve closure.

In cases where the high pressure head rise results from the second, third, or a later cavity collapse, some of the basic assumptions do not hold rigidly any longer. Thus, in reality, the cavity may not be localized to a point anymore, but could extend over a considerable distance. Therefore in such cases the actual pressure head rise is probably somewhat smaller than that indicated by the curves.

**How to avoid water column separation**

Too high an elevation of the high point is the primary cause for water column separation. Such a high point is most critical near the pump end of the pipeline.

Pipeline constant  $\rho$  is the most important of pipe parameters when water column separation is a problem. A high  $\rho$  value resulting from a high steady state water velocity in the pipe usually causes a high pressure head rise. When calculating the economical pipe diameter, water hammer should therefore always be considered. This would result in a lower initial steady state velocity than otherwise would be the case.

Of pump parameters, the inertia of the motor can be varied without undue change in cost. Ultralight modern electric motors should be avoided whenever water column separation could occur. Column separation is eliminated at the majority of the points studied when the inertia parameter  $\tau$  of the pumping unit is 0.50 or more. In addition, a lower steady state speed of the unit could be considered. This results in a heavier pump motor and a larger  $\tau$  value.

To eliminate the danger of particularly high pressure head rises resulting from column separation, avoid the areas of sharp pressure head peaks that occur in high points located at the mid-length and at the three-quarter point of pipelines with extremely low  $\tau$  values.

Finally, the economical analysis will indicate whether or not it is advisable to lower or to eliminate the high point, increase the pipe diameter, increase the inertia of the motor, strengthen the pipe to withstand the pressure head rise, provide protective devices, or to use a combination of these provisions.

**Pumping heads other than 12 m**

The graphs (Figs. 8-20) have been drawn for a total pumping head of  $H_r = 12.0$  m (39.37 ft) and a barometric pressure head of  $H_b = 9.6$  m (31.50 ft). These graphs can be used for other pumping heads  $H_r$  and barometric heads  $H_b$  in cases where the variables  $\rho$ ,  $h_f$ ,

TABLE 1. Relative height of high point

$r_2$	$Y$ , m (ft)
For $H_r = 9$ m (29.53 ft)	
1.47	13.2 (43.31)
1.27	11.4 (37.40)
1.07	9.60 (31.50)
0.87	7.80 (25.59)
For $H_r = 12$ m (39.37 ft)	
1.20	14.4 (47.24)
1.00	12.0 (39.37)
0.80	9.60 (31.50)
0.60	7.20 (23.62)
For $H_r = 15$ m (49.21 ft)	
1.04	15.6 (51.18)
0.84	12.6 (41.34)
0.64	9.60 (31.50)
0.44	6.60 (21.65)

NOTE:  $H_b = 9.6$  m (31.50 ft)

$\tau$ , and  $r_2$  are changed accordingly. The changes to  $\rho$ ,  $h_f$ , and  $\tau$  do not need any explanation. The new value for  $r_2$  is calculated as follows:

$$[11] \quad r_2^{H_r, H_b} = r_2^{12, 9.6} - \frac{H_b^{9.6}}{H_r^{12}} + \frac{H_b}{H_r}$$

in which  $r_2^{12, 9.6}$  = relative elevation of the high point in a pumping system with pumping head  $H_r$  and barometric pressure head  $H_b$  equal to 12 m (39.37 ft) and 9.6 m (31.50 ft) respectively,  $r_2^{H_r, H_b}$  = actual relative elevation of the high point in a pumping system with the pumping head  $H_r$  other than 12 m and a barometric pressure head  $H_b$  other than 9.6 m.

The graphs are based on relative high point elevation  $r_2$  values of 0.6, 0.8, 0.9, 1.0, and 1.2. The corresponding  $r_2$  values for 9 m (29.53 ft) and 15 m (49.21 ft) head pumping systems are shown in Table 1. Below the  $r_2$  values in this table are printed the corresponding high point elevations  $Y$  measured in feet from the sump level. Intermediate values for both  $r_2$  and  $Y$  can be interpolated.

**Example**

Consider the installation shown in Fig. 1 having the following data:  $H_r = 15$  m,  $H_b = 9$  m,  $H_f + H_1 + H_v = 3$  m,  $h_f = 0.20$ ,  $\rho = 5.0$ ,  $\tau = 0.47$ ,  $r_1 = 0.25$ , and  $r_2^{15, 9} = 0.7$ .

Find (a) the relative elevation of high point  $r_2^{12, 9.6}$  to enter the graphs of Figs. 8-20, which are based on  $H_r = 12$  m and  $H_b = 9.6$  m; and (b) the maximum pressure head rise caused by water column separation.

The relative elevation of high point is

$$r_2^{12, 9.6} = r_2^{15, 9} + \frac{H_b^{9.6}}{H_r^{12}} - \frac{H_b^9}{H_r^{15}} = 0.70 + \frac{9.6}{12} - \frac{9}{15} = 0.90$$

For the maximum pressure head rise, a relative value of 1.50 is read from Fig. 12 for  $h_f = 0.2$ ,  $\rho = 5.0$ , and  $\tau = 0.47$ . Therefore a maximum pressure head rise of  $1.50(15) = 22.5$  m must be allowed for when calculating the required strength of the pipe.

### Conclusions

(1) Water column separation occurring in a high point can yield a dangerous pressure head rise in the pipeline. In the studied range of  $\rho$  and  $\tau$ , water column separation occurs in all high points when low  $\tau$  values are combined with some  $\rho$  value between 2 and 16.

(2) The vertical elevation of the high point has the primary influence on water column separation and on the resulting maximum pressure head rise.

(3) Sharp pressure head peaks occur at nearly all high point locations studied. The magnitude and the location of the pressure head peaks on the  $\rho$ - $\tau$  plane depend on the elevation and the horizontal location of the high point and on pipe friction and pump inertia. Pressure head rises higher than nine times the initial steady state pumping head can occur in these cases.

(4) Very little or no water column separation occurs in the high points considered when low  $\rho$  values are combined with high  $\tau$  values.

(5) Water column separation does not always signal a danger for the pipeline. In many cases, column separation only marginally increases the pressure head rise above that produced by check valve closure. However, the hissing and thumping noise that may occur may be objectionable.

(6) Large friction in general reduces the pressure head rise caused by water column separation and sometimes eliminates the separation.

(7) Low head installations are more susceptible to water column separation than high head installations.

### Acknowledgements

The authors are grateful to the Natural Sciences and Engineering Research Council of Canada for financial support of the research, and to Mr. R. Brun, who did the large amount of drafting involved.

- ALLIEVI, L. 1925. Theory of water hammer (translated by E. E. Halmos). Riccardo Garoni, Rome.
- BERGERON, L. 1961. Water hammer in hydraulics and wave surges in electricity. John Wiley & Sons, New York, NY.
- CHAUDHRY, M. H. 1979. Applied hydraulic transients. Van Nostrand Reinhold, New York, NY.
- DONSKY, B. 1961. Complete pump characteristics and the effects of specific speeds on hydraulic transients. Journal of Basic Engineering, **83**, pp. 685-699.
- GANDENBERGER, W. 1950. Grundlagen der graphischen Ermittlung der Druckschwankungen in Wasser versorgung-

sleitungen. Verlag von R. Oldenbourg, Munich, Germany.

KINNO, H., and KENNEDY, J. F. 1965. Water hammer charts for centrifugal pump systems. ASCE Journal of the Hydraulics Division, pp. 247-270.

MARCHAL, M., FLESCH, G., and SUTER, P. 1965. The calculation of water hammer by means of the digital computer. International Symposium on Water Hammer in Pumped Storage Projects, ASME, pp. 168-200.

WYLIE, E. B., and STREETER, V. L. 1983. Fluid transients. FEB Press, Ann Arbor, MI.

### List of symbols

$a$	water hammer wave velocity (m/s)
$D$	pipe diameter (m)
$f$	friction factor
$g$	acceleration of gravity (m/s <sup>2</sup> )
$H$	transient pumping head (m)
$H_b$	barometric pressure head (m)
$H_f$	head loss due to wall friction (m)
$H_l$	sum of local losses (m)
$H_0$	static head (m)
$H_r$	rated pumping head (m)
$H_v$	velocity head (m)
$h$	relative transient pumping head
$h_f$	relative head loss
$K$	local loss coefficient
$K_1$	pump constant
$L$	pipe length (m)
$N$	transient pump speed (rpm)
$N_r$	rated pump speed (rpm)
$Q$	transient pump discharge (m <sup>3</sup> /s)
$Q_r$	rated pump discharge (m <sup>3</sup> /s)
$r_1$	relative horizontal location of high point
$r_2$	relative elevation of high point
$T$	transient pump torque (kN·m)
$T_r$	rated pump torque (kN·m)
$t$	time (s)
$t'$	relative time
$\Delta t$	time interval (s)
$v$	relative transient pump discharge
$V_0$	initial steady state velocity (m/s)
$WR^2$	moment of inertia of rotating parts ((kg·m <sup>3</sup> )/s <sup>2</sup> )
$w$	unit weight of water (kN/m <sup>3</sup> )
$X$	distance from pump end (m)
$Y$	vertical distance from water surface to high point (m)
$\alpha$	relative pump speed
$\Delta\alpha$	relative speed reduction
$\beta$	relative pump torque
$\beta_a$	average relative torque
$\eta_r$	pump efficiency at rated condition
$\mu$	time constant (s)
$\rho$	pipeline constant
$\tau$	inertia constant